IOPscience iopscience.iop.org

Home Search Collections Journals About Contact us My IOPscience

AlGaN/GaN multiple quantum wells grown on facet-controlled epitaxial lateral overgrown GaN/sapphire templates

This article has been downloaded from IOPscience. Please scroll down to see the full text article.

2007 J. Phys.: Condens. Matter 19 056005

(http://iopscience.iop.org/0953-8984/19/5/056005)

View the table of contents for this issue, or go to the journal homepage for more

Download details:
IP Address: 129.252.86.83
The article was downloaded on 28/05/2010 at 15:56

Please note that terms and conditions apply.

INSTITUTE OF PHYSICS PUBLISHING JOURNAL OF PHYSICS: CONDENSED MATTER

J. Phys.: Condens. Matter **19** (2007) 056005 (10pp) doi:10.1088/0953-8984/19/5/056005

AlGaN/GaN multiple quantum wells grown on facet-controlled epitaxial lateral overgrown GaN/sapphire templates

H L Zhou[1,3], **S J Chua**[2,3], **S Tripathy**[2], **N L Yakovlev**[2], **L S Wang**[2] **and W Liu**[2]

[1] Department of Physics, National University of Singapore, 2 Science Drive 3, 117542, Singapore
[2] Institute of Materials Research and Engineering, 3 Research Link, 117602, Singapore

E-mail: Zhouhailong@nus.edu.sg and elecsjc@nus.edu.sg

Received 1 August 2006, in final form 15 November 2006
Published 15 January 2007
Online at stacks.iop.org/JPhysCM/19/056005

Abstract

Epitaxial lateral overgrowth of GaN with $(11\bar{2}2)$ facets was realized by metal–organic chemical vapour deposition on GaN/sapphire (0001) substrates with an SiO_2 stripe mask. After wet etching of the mask, periodic AlGaN/GaN multiple quantum wells (MQWs) were grown on the whole surface. Cross section transmission electron microscopy showed that the average growth rate on the $(11\bar{2}2)$ facet is lower than on the (0001) plane. The concentration of Al of AlGaN/GaN MQWs was higher on the (0001) facet than on the $(11\bar{2}2)$ surface, as measured by secondary ion mass spectrometry and high resolution x-ray diffraction (HR-XRD). Micro-Raman scattering spectroscopy revealed a significant relaxation of compressive stress in the laterally overgrown GaN. Micro-photoluminescence spectra confirmed quantum confinement of electrons in MQWs. The achieved optical quality of MQWs on the $(11\bar{2}2)$ facet is comparable with that on the (0001) plane.

1. Introduction

Semiconductors from the GaN family, such as $In_xGa_{1-x}N$ and $Al_xGa_{1-x}N$, are widely used for light emitting devices (LED) in the green and blue spectral range [1, 2]. Their common part is a layer with multiple quantum wells (MQWs) to trap electrons and holes for their efficient recombination. The performance of these LEDs can be improved, if their design overcomes two main issues.

First, there is a high dislocation density of about 10^9–10^{10} cm^{-2} in GaN grown on traditional substrates like Al_2O_3 (sapphire) because of large lattice mismatch. Possible solutions are to use better matching substrates like SiC or AlN [3], which are usually more

[3] Authors to whom any correspondence should be addressed.

expensive, or to grow GaN using the epitaxial lateral overgrowth (ELO) technique. In the latter case, a mask of a foreign material, usually SiO_2, is deposited on a GaN seed layer and the growth is resumed on the openings of the mask. Thus GaN growing laterally over the mask has lower dislocation density than the seed layer.

Second, when the GaN growth surface is the (0001) plane, planar strain induced by the different lattice constants of the GaN quantum wells and the AlGaN barrier layers gives rise to strong internal piezoelectric fields [4]. This leads to a local separation of electrons and holes in these quantum wells, poor overlap of electron and hole wavefunctions, long radiative lifetimes [5], and low internal quantum efficiencies [6, 7], where competing non-radiative channels are always present in the device structures. Reduction of electrostatic fields is possible by growing the structures on the non-polar or semi-polar plane of sapphire, e.g. on the *r*-plane [8] or the *a*-plane, where GaN grows on the $(10\bar{1}2)$ or $(11\bar{2}0)$ direction [9, 10]. Other approaches make use of more exotic substrates such as $LiAlO_2$ [11], on which pure *m*-plane GaN$(1\bar{1}00)$ growth was achieved. However, on these substrates, it is difficult to achieve high crystalline quality GaN, and device performance cannot compete with that obtained on the commonly used *c*-plane of sapphire.

A technique which can help to overcome both problems is facet-controlled epitaxial lateral overgrowth (FACELO). It is realized by starting the epitaxial growth on the (0001) plane and tuning the growth conditions to develop other facets, e.g. $(1\bar{1}01)$ and $(11\bar{2}2)$, on ELO stripes [12]. FACELO GaN was used as a substrate to grow InGaN/GaN MQWs with a reduced piezoelectric field [13].

In this work, AlGaN/GaN MQWs on FACELO GaN$(11\bar{2}2)$ facets were grown for the first time. Scanning electron microscopy (SEM) and cross-sectional transmission electron microscopy (TEM) were used to characterize the morphology and structure of the MQWs. The concentration of Al was measured using secondary ion mass spectroscopy (SIMS). Optical properties of MQWs on individual $(11\bar{2}2)$ and (0001) facets were studied using micro-Raman scattering and micro-photoluminescence (PL) spectroscopy. The results showed that the optical quality of MQWs on the FACELO GaN$(11\bar{2}2)$ facet is comparable with that of MQWs on the (0001) plane, which is used traditionally for opto-electronic devices.

2. Experimental details

To prepare ELO GaN, a 2.0 μm thick GaN layer was first deposited on a *c*-plane sapphire substrate by MOCVD. Trimethyl metals and ammonia (NH_3) were respectively used as precursors for group III and N, and H_2 was used as carrier gas. An about 100 nm thick SiO_2 mask was patterned into stripes oriented in the $\langle 1\bar{1}00\rangle$ direction of GaN, defining a 4 μm wide opening with a period of 13 μm. After 30 min of regrowth on these templates, ELO GaN with $\{11\bar{2}2\}$ facets was selectively overgrown. The growth temperature was 950 °C and reactor pressure was 500 Torr. After the SiO_2 mask was removed by HF solution, ten periods of AlGaN/GaN MQWs were grown on the whole surface. The target Al composition in the barriers was 10%. The growth temperature was about 1000 °C, the reactor pressure was kept at 60 Torr, the flow rates of TMGa and TMAl were about 30 and 80 sccm and the growth times of the well and barriers were 12 and 18 s, respectively.

The morphologies of the layers and cleaved cross-sections were studied with a JEOL 6700 FE SEM at electron energy 5 keV. The internal structure of the MQWs was studied with a Philips CM300 FEG TEM. The composition of the epitaxial layers was measured using secondary ion mass spectrometry (SIMS) in a ToF-SIMS-IV instrument. The depth profiles were obtained using 3 keV Ar^+ for sputtering and 25 keV $^{69}Ga^+$ beam for mass analysis, both at 45° incidence. Focusing of the analysis beam provided lateral resolution better than

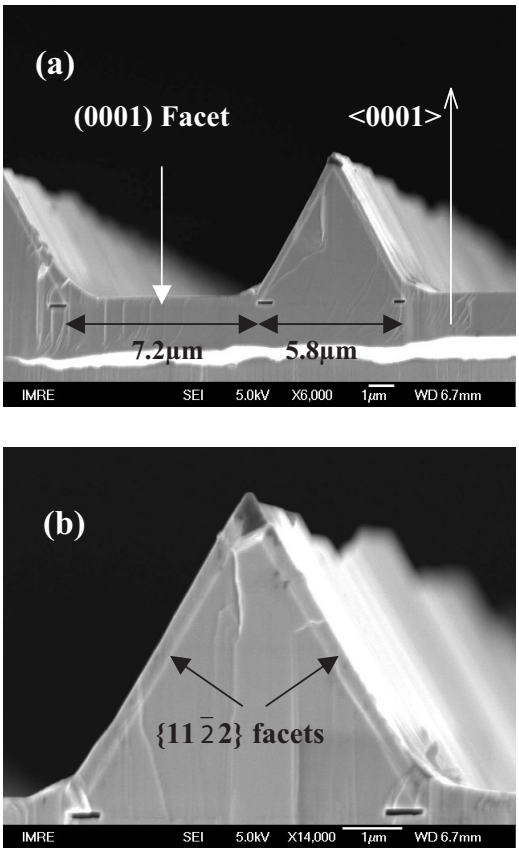

Figure 1. Cross-sectional SEM of the FACELO GaN sample. AlGaN/GaN MQWs are within 140 nm under the surface. (a) and (b) are SEM images from the same sample at different magnification.

1 μm. HR-XRD was also performed on the AlGaN/GaN MQW sample using a high resolution Philips MRD system. The extent of stress relaxation in the faceted GaN stripes and flat GaN was evaluated by micro-Raman scattering spectroscopy with a 514.5 nm excitation line from an Ar ion laser. Lateral resolution of Raman measurements was about 1 μm. The PL spectra were recorded at room temperature using a 325 nm excitation line with a lateral resolution of 2 μm (Renishaw 2000 set-up).

3. Structure and composition of MQWs

The morphology of FACELO GaN has the shape of a prism with a triangular cross-section, as seen from the SEM image in figure 1. The triangular cross-sections are about 5 μm high and 5.8 μm wide and the spacing between them is about 7.2 μm. The roughness of the (11$\bar{2}$2) surface seen in figure 1 is due to the short growth time of ELO GaN. The dark rectangular shaped holes at the base of the triangles of ELO GaN are the voids formed due to removal of the SiO_2 mask.

Figure 2 shows the cross-sectional TEM images of the AlGaN/GaN MQWs grown simultaneously on the (11$\bar{2}$2) facets and on the *c*-planes. From figure 2(a), it is seen that the ten

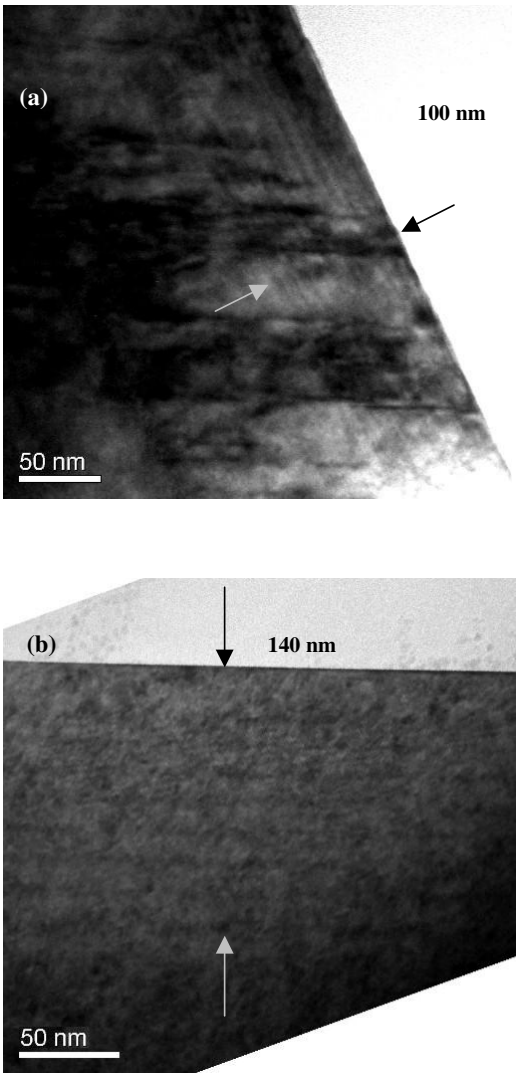

Figure 2. Cross-sectional TEM images of the AlGaN/GaN MQWs: (a) taken along the $(11\bar{2}2)$ faceted MQWs; (b) taken along the *c*-plane MQWs.

periods of AlGaN/GaN MQWs are grown on the $(11\bar{2}2)$ facet successfully with total thickness of approximately 100 nm. From figure 2(b), we observed *c*-plane or (0001)-oriented MQWs with total thickness 140 nm. The different growth rates of MQWs on these facets are evident from the structural analysis. As the GaN growth rates are found to be 1.4 times higher along the *c*-direction, the well and barrier width in these planes are larger than those on the $(11\bar{2}2)$ facets. The well to barrier ratio was determined by the growth time. The well and barrier thicknesses are approximately 4 and 6 nm respectively on the $(11\bar{2}2)$ facets and about 5.5 and 8.5 nm respectively on the *c*-plane.

The growth rate on the two facets is controlled by two competing factors. First, the $(11\bar{2}2)$ surface has a lower number of coordinated surface atom bonds than those on the (0001) surface [15]. For III–V semiconductors, surface atoms always prefer to attach at positions with

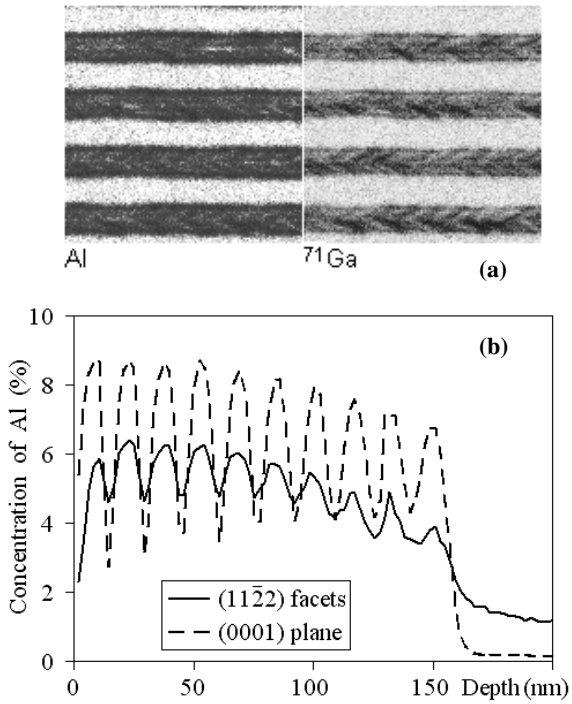

Figure 3. SIMS results from AlGaN/GaN MQWs: (a) maps of Al and ^{71}Ga on four stripes; the analysis area is 50 μm × 50 μm; (b) depth profiles of Al concentration of the two different facets.

the highest possible coordination number since they are positions of minimum energy. Thus, the sticking coefficient of Al and Ga adatoms on the (0001) surface is higher to result in a higher growth rate. Second, (11$\bar{2}$2) facet morphology is different; it has more incorporation sites due to a rougher surface related to the presence of steps and kinks, which can increase the growth rate slightly. The results indicate that the dominant factor for the difference of the growth rates is the different coordination of adatoms.

To determine the Al composition in the AlGaN/GaN MQWs, SIMS depth profiling was carried out. During the acquisition of SIMS data, each secondary ion reaching the detector is stored in a raw data file. From this file, it is possible to reconstruct the mass spectra, depth profiles, or mass-resolved images (chemical maps) as shown in figure 3. The chemical maps show ions of particular mass originating from the scanned pixels, where the white region corresponds to higher and the dark region to lower intensity. On the maps of both Al and Ga, shown in figure 3(a), the *c*-plane facets appear as bright and ELO prisms as dark. This is due to the decrease of sputtering yield at glancing angles and curvature of electric field accelerating secondary ions from the inclined surfaces. The typical chevron pattern on ELO is due to the roughness of (11$\bar{2}$2) facets, which is also evident from figure 1. The depth profiles shown in figure 3(b) were reconstructed on selected areas of the scan corresponding to the *c*-plane (dashed line) and ELO regions (solid line). Ten periods of the multiple quantum wells are seen on both areas.

To convert the ratio of Al to ^{71}Ga SIMS intensities to the concentration of Al, a flat $Al_{0.1}Ga_{0.9}N$ layer on GaN/sapphire(0001) was used as a reference sample. It is seen that the average content of Al is around 6% on both facets, but the amplitude of the oscillations is

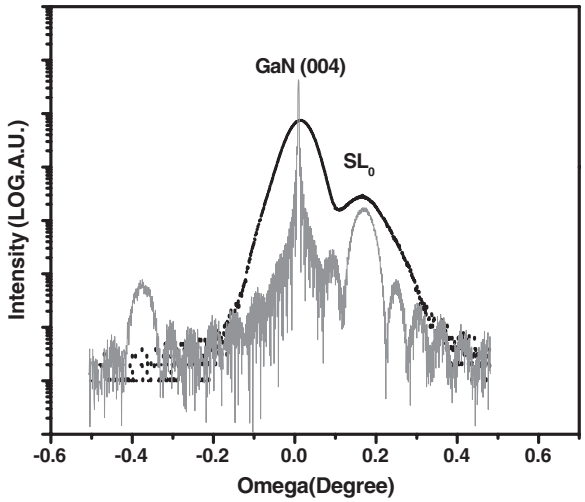

Figure 4. High resolution x-ray diffraction $\omega/2\theta$ experimental (· · · · · ·) and calculated (— —) triple-axis symmetrical scans near the (0004) GaN diffraction peak taken on the AlGaN/GaN MQWs grown on the FACELO GaN templates.

different. On the flat *c*-plane MQWs, the contrast is determined by SIMS depth resolution, which is estimated to be around 3 nm. On the $(11\bar{2}2)$ facets, the contrast is lower due to the roughness of these facets, so that the rising and falling slopes of the chevrons are sputtered by Ar^+ beam with different rates. Thus, the oscillations decay faster than on the *c*-plane and there is a tail of Al after MQWs. SIMS results confirm that Al incorporation occurs on both the *c*-plane and $(11\bar{2}2)$ facet and the incorporation rate is the same within 10% accuracy. Two factors can affect the incorporation rate of Al. Firstly, the $(11\bar{2}2)$ surface has a lower number of coordinated surface atom bonds, which decreases Al incorporation with respect to the (0001) surface [15]. Secondly, because the MQWs were grown at higher temperature than preceding GaN, there is a residual tensile stress, which is lower in the prism than in the (0001) seed layer. This can increase Al incorporation on the $(11\bar{2}2)$ facets. However, SIMS results cannot show which factors have significant effects on the Al content difference between the two facets. Then we use high resolution XRD to determine the Al composition in the AlGaN/GaN MQWs; the XRD profile of AlGaN/GaN MQWs grown on the FACELO GaN templates (figure 4) was taken in the vicinity of the (0004) diffraction. Only one satellite peak was seen; this may be induced by the micro-size stripe line pattern and the roughness of the $(11\bar{2}2)$ facets, so we cannot use these data to deduce both quantum well thickness and Al content. But Al composition can be estimated using the quantum well thickness characterized by TEM. The Al content of our case of AlGaN/GaN MQWs grown on the FACELO GaN templates was 12.3% by a fit using the dynamical diffraction theory. Compared with the SIMS results, this indicates that we have more Al content of the AlGaN/GaN MQWs on the (0001) facets than the $(11\bar{2}2)$ surface.

4. Optical properties of MQW

The optical properties of the AlGaN/GaN MQWs were investigated by micro-Raman scattering and micro-PL spectroscopy. Raman scattering was used to examine the relaxation of compressive strain, which is due to the difference of thermal expansion and lattice constants of GaN and sapphire. Raman spectra of the samples were recorded from different regions of the

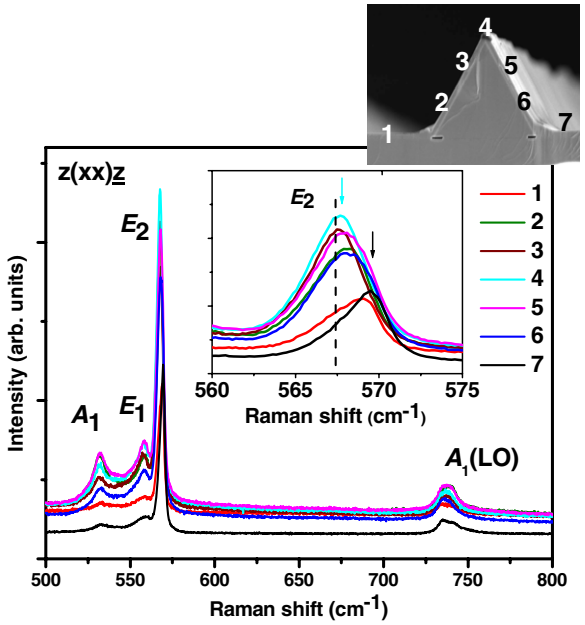

Figure 5. Room temperature micro-Raman spectra recorded from the AlGaN/GaN MQWs at different positions are marked in the inset of the SEM image. The dashed line in the inset indicates the peak position recorded from the strain-free freestanding GaN.

(This figure is in colour only in the electronic version)

facets and are shown in figure 4. The E_2-high mode in the Raman spectra was used to measure the strain, because it has been proven to be particularly sensitive to the biaxial stress in GaN epitaxial layers [14]. Along the c-direction of the seed layer, the E_2-mode is shifted to higher frequencies with respect to the standard value of 567.5 cm^{-1} recorded from a 400 μm thick freestanding GaN substrate. The shift is about 2.0 ± 0.2 cm^{-1} on the seed layer GaN and only 0.4 ± 0.2 cm^{-1} on top of ELO GaN. Intermediate values were recorded along $(11\bar{2}2)$ facets. Using the proportionality factor of 4.2 cm^{-1} GPa^{-1} for hexagonal GaN [16], we obtain values of residual stress of 0.47 ± 0.05 GPa in the seed layer GaN and a stress variation of 0.09–0.17 GPa on the $(11\bar{2}2)$ facet of the ELO GaN (figure 5). Thus the average strain relaxation difference between the two facets is about 0.3 GPa. Because visible Raman excitation probes the whole crystal, no conclusive evidence of Al content can be found in the two different facets due to the small Al concentration in MQWs.

In PL experiments, the penetration depth of the excitation light is less than 200 nm, hence most of the PL emission originates from the MQWs. The contribution of the GaN substrate is discussed at the end of the next paragraph. In the PL spectra shown in figure 6, the peaks from both facets show a blue shift with respect to bulk GaN and the shift is higher for the $(11\bar{2}2)$ facet. The shift of PL peaks can be caused by three factors.

First, compressive stress shifts the peaks to higher energy. The value of 21 ± 3 meV GPa^{-1} was used as the factor of the PL peak shift in GaN induced by stress [17], and we calculate that the stress component of the shift is about 3–4 meV for ELO GaN and 10 meV for seed layer GaN with respect to the bulk. However, the peak from MQWs on $(11\bar{2}2)$ facets is actually on the higher energy side of that of (0001) facets, hence the stress effect is compensated by other stronger effects. The stress-induced shift must be present in PL spectra of ELO GaN substrate,

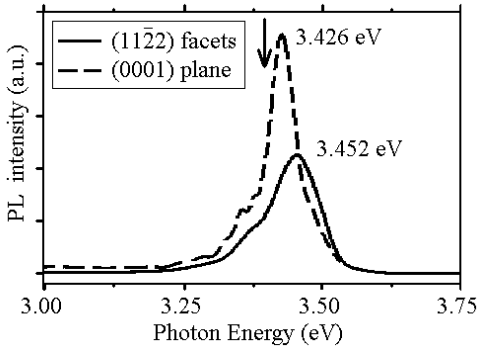

Figure 6. Room temperature micro-PL spectra recorded from AlGaN/GaN MQWs at two different facets. The arrow indicates the peak position at 3.390 eV in bulk GaN.

but there are no features at those positions, and thus the contribution of the substrate to the PL intensity is really small.

Second, quantum confinement of charge carriers in quantum wells must give a blue-shift, which is higher for thinner wells. As a rough estimation, we use the electron effective mass as 0.2 m_0 and the formula for the ground state energy in a deep well $\sim h^2/8\ ma^2$, where h is the Planck constant, m is the electron mass and a is the well width. Thus roughly we can obtain a shift of about 117 meV in the 4 nm wide wells on the (11$\bar{2}$2) facet and 62 meV in 5.5 nm wide wells on the (0001) facet.

Third, GaN with wurtzite structure has a singular polar [0001] axis, and this creates an electrostatic field along the [0001] axis due to the spontaneous and piezoelectric polarization [18, 19]. According to the quantum-confined Stark effect [20, 21], the PL peak energy of (0001)-faceted GaN will show a red-shift compared to non-polar directions. In the case of AlGaN/GaN MQWs grown on *R*-plane (11$\bar{2}$2) sapphire substrates by molecular-beam epitaxy, the peak transition energies showed a significant blue-shift when compared to the (0001) MQWs [9]. According to a theoretical study of the orientation dependence of piezoelectric effects in InGaN/GaN quantum wells [22], we can get a similar estimation of piezoelectric fields in our AlGaN/GaN quantum wells, which are about 0.2 MV cm^{-1} on the (0001) facet and -0.08 MV cm^{-1} on the (11$\bar{2}$2) facet; the signs of these values are opposite in accordance with [22]. The second contribution to the electric field is due to the difference in spontaneous polarization of the layers, which has a considerable value of -0.55 MV cm^{-1} in AlGaN/GaN quantum wells on the *c*-plane, while it could be neglected in InGaN/GaN quantum wells [22]. In the direction normal to the ELO facet, the component of spontaneous polarization is -0.27 MV cm^{-1}, thus together with the piezoelectric contribution the field is -0.35 MV cm^{-1}. On the *c*-plane, these contributions are in opposite directions, thus the total field is also -0.35 MV cm^{-1}. With these values, the estimation of the quantum-confined Stark effect as in [22] gives a red-shift of the transition energy by an amount of -37 meV in 5.5 nm wells on the (0001) facet and -27 meV in 4 nm wells on the (11$\bar{2}$2) facet. So this factor also contributes to the blue-shift of PL from GaN/AlGaN MQWs on the semipolar (11$\bar{2}$2) facet with respect to the (0001) facet. Assuming that the three contributions of PL peak shift can be added, we can estimate the overall shifts, as shown in table 1. In the calculation of quantum confinement of charge carriers in quantum wells, we are not including the difference of the barrier heights between both facets. With our HR-XRD results, the (11$\bar{2}$2) facets show higher Al content than the (0001) facets, that means it will induce a larger blue-shift compared

Table 1. Estimated contributions toward the peak shift in PL spectra from ELO AlGaN/GaN MQWs on two facets.

		Contributions (meV)			Peak shift (meV)	
Facet	Well width (nm)	Thermal strain	Quantum confinement	Stark effect	Calculated	Measured
(0001)	5.5	10	62	−37	35	36
$(11\bar{2}2)$	4	4	117	−27	94	62

to the AlGaN/GaN MQWs on the (0001) facets. This maybe explains why we have a large discrepancy in PL shift between the theoretical and experimental values for $(11\bar{2}2)$ facet in table 1. Hence in our case the main contribution toward the blue-shift of PL from $(11\bar{2}2)$ facets is the quantum confinement effect in MQWs.

The width of this PL peak from MQWs on the $(11\bar{2}2)$ facets is larger than that from (0001) faceted MQWs. Because the main factor for the PL peak shift is quantum confinement of electrons, the peak broadening must be attributed first of all to random variations of quantum well width, which is more significant for rougher substrate and thinner wells. We attribute the broadening to the well-size fluctuation in the non-polar AlGaN/GaN MQWs.

The PL peak intensity of the $(11\bar{2}2)$ faceted MQWs is weaker and about half of the intensity recorded from (0001) MQWs. Because collection of emitted light to the PL spectrometer from inclined $(11\bar{2}2)$ facets is half that from (0001) facets, these intensities show that internal emission efficiency is similar on both facets. In GaN-based materials, usually a roughened or porous surface shows higher PL intensity due to light extraction related to multiple-scattering events of emitted photons. However, from inclined surfaces the collection efficiency of the side wall scattered photons is lower. These results show somewhat comparable optical properties of AlGaN/GaN MQWs grown on (0001) and on $(11\bar{2}2)$ facets by the FACELO method, in contrast to the low quality of MQWs grown directly on $(11\bar{2}2)$ substrates. Such structures show promising feasibility for realizing stronger oscillator strength for UV/blue colour light emitting diodes (LEDs) owing to the suppression of piezoelectric fields grown on FACELO GaN/sapphire templates.

5. Conclusions

Successful growth of AlGaN/GaN MQWs was achieved on the $(11\bar{2}2)$ facets of ELO GaN. Periodic MQW structure was confirmed by TEM and SIMS. TEM showed that the average growth rate on the (0001) facet is lower than on the $(11\bar{2}2)$ plane by a factor of 0.7. SIMS showed that the concentration of Al is the same on both facets. Micro-Raman scattering revealed that there is a relaxation of compressive stress in FACELO GaN when compared to the case of the (0001) plane. Micro-photoluminescence spectra showed a blue-shift from the $(11\bar{2}2)$ facet with respect to the *c*-plane. This is in agreement with quantum confinement of electrons. Comparable PL properties on both facets indicated high optical quality of MQWs on the $(11\bar{2}2)$ facet.

Acknowledgments

The authors acknowledge support from the NUS Academic Research Fund. We would like to thank Ms Chow Shue Yin and Ms Yong Anna Marie for their help in TEM characterization. We would also like to thank Huang Teng Chuan from Hwa Chong J C for help in SIMS measurements.

References

[1] Monemar B 1974 *Phys. Rev.* B **10** 676–81
[2] Nakamura S, Senoh M, Nagahama S, Iwasa N, Yamada T, Matsushita T, Kiyoku H, Sugimoto Y, Kozaki T, Umemoto H, Sano M and Chocho K 1998 *Appl. Phys. Lett.* **72** 211–3
[3] Gaska R, Chen C, Yang J, Kuokstis E, Khan A, Tamulaitis G, Yilmaz I, Shur M S, Rojo J C and Schowalter L J 2002 *Appl. Phys. Lett.* **81** 4658–60
[4] Bernardini F, Fiorentini V and Vanderbilt D 1997 *Phys. Rev.* B **56** R10024–7
[5] Langer R *et al* 1999 *Appl. Phys. Lett.* **74** 3827–9
[6] Deguchi T, Sekiguchi K, Nakamura A, Sota T, Matsuo R, Chichibu S and Nakamura S 1999 *Japan. J. Appl. Phys.* 2 **38** L914–6
[7] Nishida T and Kobayashi N 1999 *Compound Semicond.* **5** 12–5
[8] Takeuchi T, Amano H and Akasaki I 2000 *Japan. J. Appl. Phys.* 1 **39** 413–6
[9] Ng H M 2002 *Appl. Phys. Lett.* **80** 4369–71
[10] Craven M D, Lim S H, Wu F, Speck J S and DenBaars S P 2002 *Appl. Phys. Lett.* **81** 1201–3
[11] Waltereit P, Brandt O, Ramsteiner M, Uecker R, Reiche P and Ploog K H 2000 *J. Cryst. Growth* **218** 143–6
[12] Miyake H, Motogaito A and Hiramatsu K 1999 *Japan. J. Appl. Phys.* 2 **38** L1000–2
[13] Nishizuka K, Funato M, Kawakami Y, Fujita S, Narukawa Y and Mukai T 2004 *Appl. Phys. Lett.* **85** 3122–4
[14] Harima H 2002 *J. Phys.: Condens. Matter* **14** R967–93
[15] Ruterana P, Albercht M and Neugebauer J 2003 *Nitride Semiconductors: Handbook on Materials and Devices* (New York: Wiley–VCH) pp 310–11
[16] Kisielowski C, Kruger J, Ruvimov S, Suski T, Ager J W, Jones E, Liliental Z, Rubin M and Weber E R 1996 *Phys. Rev.* B **54** 17745–53
[17] Zhao D G, Xu S J, Xie M H, Tong S Y and Yang H 2003 *Appl. Phys. Lett.* **83** 677–9
[18] Fiorentini V, Bernardini F, Della Sala F, Di Carlo A and Lugli P 1999 *Phys. Rev.* B **60** 8849–58
[19] Bykhovski A D, Gelmont B L and Shur M S 1997 *J. Appl. Phys.* **81** 6332–8
[20] Mendez E E, Bastard G, Chang L L, Esaki L, Morkoc H and Fischer R 1982 *Phys. Rev.* B **26** 7101–4
[21] Bastard G, Mendez E E, Chang L L and Esaki L 1983 *Phys. Rev.* B **28** 3241–5
[22] Takeuchi T, Amano H and Akasaki I 2000 *Japan. J. Appl. Phys.* 1 **39** 413